JTTEES 6:85-90

Properties of Plasma-Sprayed Bond Coats

W.J. Brindley

Increasing bond coat oxidation resistance has been clearly linked to increasing durability of the ceramic layer of thermal barrier coatings (TBCs). However, recent studies have shown that significant differences in TBC life can be achieved for different bond coats that exhibit little or no difference in oxidation behavior. These data suggest that bond coat properties other than oxidation resistance can also influence TBC life. Determination of which properties affect TBC life and how they do so could be valuable in designing new, more durable TBCs. This paper reviews the results of comparative studies of the properties of three bond coat compositions that have similar oxidation behavior but different TBC lives. An analysis of the properties indicates that the thermal cycle residual stress, calculated from the coefficient of thermal expansion and the stress relaxation behavior of the three alloys, is strongly correlated to the observed differences in TBC life.

Keywords bond coat, failure, strain response, thermal barrier coatings

1. Introduction

PLASMA-SPRAYED thermal barrier coating (TBC) thermal fatigue life has been shown to be related both to oxidation of the bond coat and to thermal expansion mismatch strains (Ref 1-3). The thermal expansion mismatch strains that have received the most attention have been those between the substrate and the ceramic layer. The explanation for the lack of interest in the bond coat is that the bond coat coefficient of thermal expansion (CTE) has been shown to be relatively unimportant to the overall CTE of the ceramic layer/bond coat/substrate system, an expected result of the greater thickness of the substrate relative to the bond coat (Ref 4). Thus, development of the bond coat has traditionally aimed at higher bond coat oxidation resistance, with little attention paid to the other properties.

Although this approach has yielded significant improvements in bond coat performance (Ref 5), recent studies have indicated that other bond coat properties may also influence the thermal cycle life of TBCs. Work on high-strength bond coats by Wortman et al. (Ref 6) and an oxidation/thermal cycle life study by Brindley and Miller (Ref 7) have shown that bond coats with poorer oxidation resistance can, in some circumstances, provide longer TBC life than bond coats with better oxidation resistance.

In addition to oxidation response, bond coat properties that can reasonably be expected to influence TBC thermal cycle life include CTE, creep (stress relaxation) behavior, and elastic modulus (Ref 6, 8, 9). This paper reviews the results of comparative studies on three bond coat compositions to determine which properties influence TBC life (Ref 7, 9-11). It will be shown that the residual stress developed during thermal cycling, as determined by the bond coat CTE and stress relaxation behavior, strongly correlates to TBC life.

W.J. Brindley, NASA Lewis Research Center, Cleveland, OH 44135, USA.

2. Experimental Method

The three bond coat compositions examined throughout the series of studies were Ni-16Cr-6Al-0.3Y, Ni-18Cr-12Al-0.5Y, and Ni-35Cr-6Al-0.95Y. All the experiments were conducted on low-pressure plasma-sprayed (LPPS) deposits of the three alloys. The actual chemistries of the starting powders and the LPPS deposits are given in Table 1. The alloys will be referenced by their nominal chromium and aluminum contents—for example, 16-6 for the Ni-16Cr-6Al-0.3Y alloy. The LPPS parameters for the bond coat alloys were reported previously (Ref 7).

3. Results and Discussion

3.1 *Thermal Fatigue Life*

The most important property of a bond coat is, of course, the thermal fatigue life of the TBC system for that bond coat. The thermal fatigue life of TBCs incorporating identical air-plasma-sprayed ceramic top coats and the three different LPPS bond coats was measured in a jet-fuel-fired mach 0.3 burner rig (Ref 7). Four samples of each bond coat type were heated in the

Table 1 Chemical analyses of the starting powders and the heat-treated plasma spray deposits

	Composition, wt %								
Powder/deposit	**Ni**	**Cr**	**Al**	**Y**	**C**	**O**	**Fe**	**Co**	**Si**
16-6 powder	bal	16.5	5.8	0.30	0.008	0.015	0.032	0.074	0.15
16-6 deposit	bal	15.6	5.2	0.20	0.01	0.022	0.4	<1 ppm	0.5
18-12 powder	bal	18.5	12.2	0.45	0.017	0.025	0.038	0.038	0.021
18-12 deposit	bal	17.2	11.6	0.98	0.011	0.030	0.3	<1 ppm	0.5
35-6 powder	bal	35.0	6.0	1.08	0.014	0.019	0.18	0.038	0.065
35-6 deposit	bal	33.0	6.2	0.95	0.014	0.039	0.4	<1 ppm	0.5

burner rig flame for 6 min to a steady-state temperature of 1150 °C, followed by forced-air cooling for 4 min.

The results of the thermal fatigue testing are shown in Fig. 1. The 35-6 composition has a higher mean thermal fatigue life than the 18-12 alloy, and its mean life is higher than that of the 16-6 alloy by a factor of three. Student-Newman-Keuls analysis of the data showed that the differences in mean life were significant at the 95% confidence level, giving a life ranking as: 35-6 > 18-12 > 16-6. The mean TBC lives and 95% confidence intervals for the three bond coat alloys are shown in Fig. 1.

3.2 *Oxidation*

Based on the dramatic thermal fatigue life differences and the assumption that the lowest oxidation resistance bond coat should result in the poorest TBC life, it was expected that the 16-6 alloy would show significantly higher oxidation weight gains than the 35-6 alloy. This was not the case. Figure 2 shows the specific weight gains of freestanding coupons for isothermal oxidation at 1100 °C in air. Each of the three compositions was oxidized in three conditions: polished, grit blasted, and grit blasted plus thermal barrier coated (Ref 7). The 16-6 alloy had the lowest weight gain (best oxidation resistance) for all three surface conditions, whereas the 18-12 and 35-6 alloys had higher weight gains. This result contradicts the expected inverse relation of TBC life to bond coat oxidation weight gain. Clearly, the answer to this apparent contradiction is that bond coat properties other than oxidation influence TBC life.

It should be noted that the isothermal oxidation rate results were consistent with the trends in oxide thickness for the burner-rig-tested coupons. Furthermore, the oxide species present on all three alloys after isothermal exposure and after burner rig testing were the same. Thus, TBC life differences could not be explained on the basis of the formation of different oxides for different bond coat compositions or by a change in oxidation mechanism between isothermal and cyclic exposure (Ref 7).

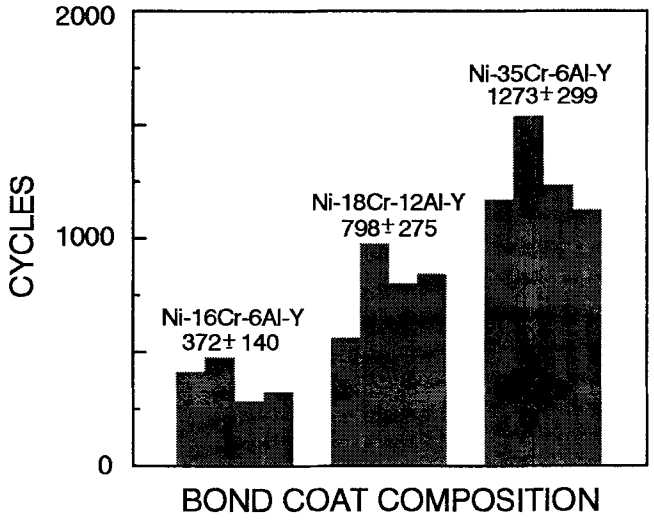

Fig. 1 Thermal cycle lives of two-layer TBCs, with 16-6, 18-12, and 35-6 bond coats, tested in a JP-5 fueled burner rig. The thermal cycle was 6 min in the flame, effectively 4 min at 1150 °C, followed by 4 min of forced-air cooling to 30 °C. The mean life and 95% confidence interval are indicated for each composition. Source: Ref 7

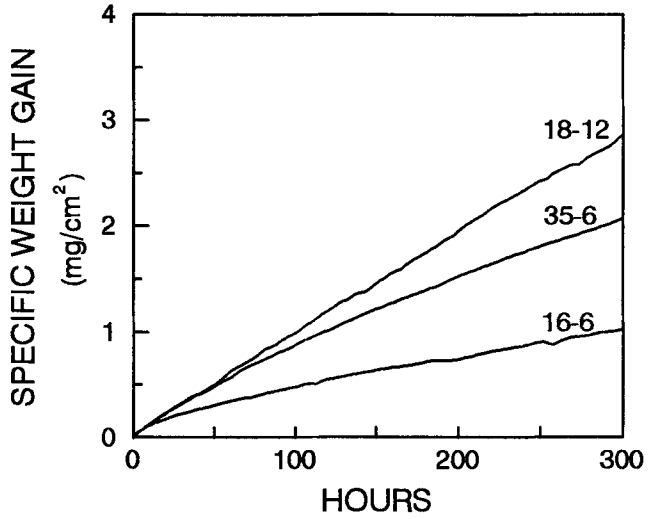

Fig. 2 Oxidative weight gains of the 16-6, 18-12, and 35-6 alloys during isothermal oxidation at 1100 °C. Curves are representative of six samples for each composition. Source: Ref 7

3.3 *Thermal Expansion*

The CTE of freestanding NiCrAlY coupons was measured as a function of temperature from 23 to 1000 °C (Fig. 3) (Ref 9). The CTE shown is the average CTE from room temperature to the temperature of interest. The 16-6 alloy exhibited a fairly smooth concave curve that had higher CTEs than the other two alloys up to approximately 900 °C. Both the 18-12 and 35-6 alloys showed dramatic increases in CTE with increasing temperature, starting at about 800 °C, and both had higher CTEs than the 16-6 alloy at 1000 °C. The CTE responses measured at other laboratories for a Ni-22Cr-10Al-Y bond coat alloy were quite similar to that found for the 18-12 alloy (Ref 12, 13). The reason for the differences in CTE response among the alloys has been discussed elsewhere (Ref 9, 12). The important features of

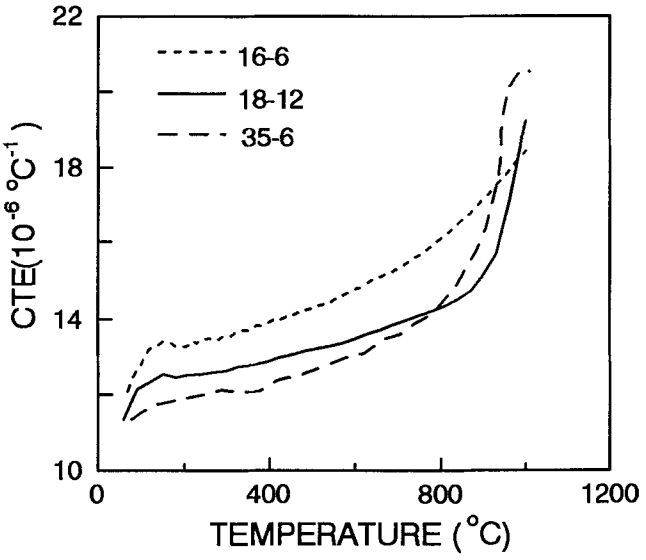

Fig. 3 Average CTE from 22 °C to the plotted temperature for the 16-6, 18-12, and 35-6 alloys. The plotted data were obtained during cooling. Source: Ref 9

these curves for this discussion are that there are significant differences in the temperature-dependent CTEs of the three alloys and that both the 18-12 and 35-6 alloys have higher CTEs than the 16-6 alloy at 1000 °C. A clearer understanding of the significance of these differences will be developed in section 3.6.

3.4 *Elastic Modulus*

The elastic modulus was measured dynamically on freestanding coupons of the three LPPS NiCrAlY alloys as a function of temperature from 23 to 1000 °C (Ref 11). The results of the measurements are shown in Fig. 4.

There were differences in the bond coat elastic modulus, especially notable at temperatures below 500 °C. However, it is clear that the bond coat moduli up to 1000 °C were quite high compared to the modulus of plasma-sprayed zirconia-yttria, shown as a range from 20 to 60 GPa in Fig. 4 (Ref 12, 13). Elastic moduli measured dynamically for plasma-sprayed Ni-22Cr-10Al-Y (Ref 12, 13) showed behavior similar to that of the 16-6 and 18-12 alloys of Ref 11. Since the elastic stress generated in the coating will be dominated by the lower-modulus material, it is evident that the ceramic layer modulus will determine the stress in the TBC up to and probably beyond 1000 °C. Noting that the bond coat modulus decreases with temperature, it may be that at the 1150 °C steady-state temperature of the burner rig test, the bond coat moduli would be low enough to control stress generation if the system remains elastic. However, as is shown in section 3.5, all three bond coats creep rapidly at temperatures above 900 °C. Therefore, the stresses will be limited by relaxation of the bond coat and not by the bond coat elastic properties.

3.5 *Stress Relaxation*

A limited amount of creep testing on plasma-sprayed MCrAlY materials has been reported (Ref 10, 13-15). Creep testing, defined as time-dependent deformation under a fixed stress (or load), will give a strong indication of how much stress relaxation will occur for a bond coat. However, the actual deformation that occurs during thermal cycling is time-dependent, inelastic deformation imposed by a fixed thermal expansion mismatch strain—in other words, stress relaxation. Stress relaxation tests were conducted on the three alloys to develop data that were directly applicable to stress relaxation during thermal cycling.

The stress relaxation tests were conducted at temperatures from 22 to 1000 °C by compressing freestanding specimens at a constant crosshead velocity until an approximately steady-state stress was attained (Ref 10). At this point the crosshead of the test machine was stopped, and the load was monitored as a function of time. Figure 5 shows the stress versus time trace for multiple tests on a single sample. Relaxation data such as in Fig. 5 were reduced to strain versus time curves, the usual practice for representing creep. It was found that the stress relaxation data and the creep data from ancillary constant-crosshead-velocity tests agreed quite closely (Ref 10). This means that creep and stress relaxation behaviors are history independent for these materials.

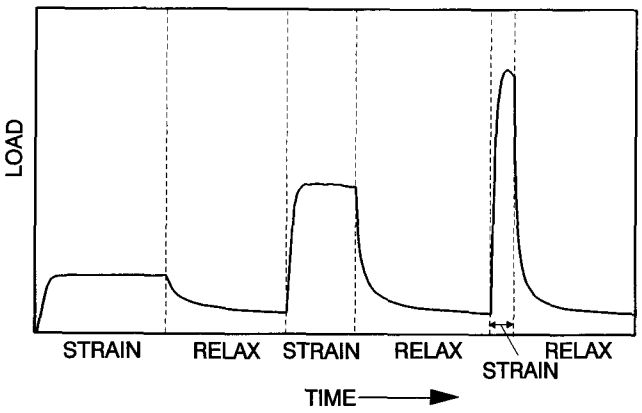

Fig. 5 Schematic of the loading and stress relaxation test sequence used to determine relaxation behavior for multiple starting stresses for a single sample. Source: Ref 10

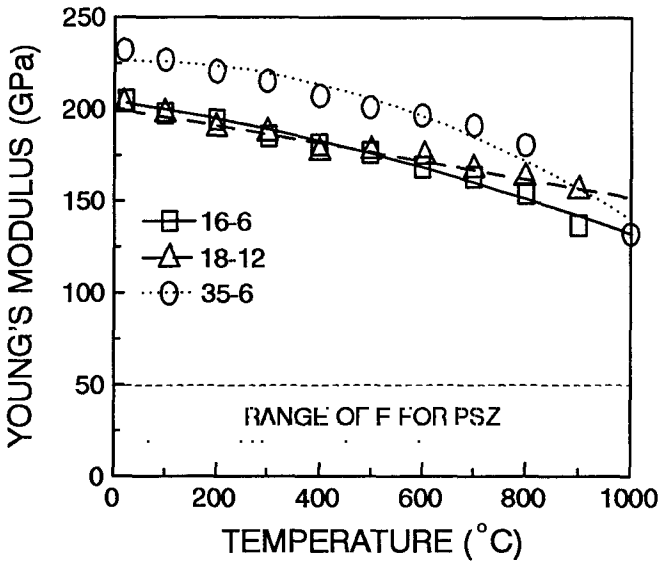

Fig. 4 Dynamic Young's modulus as a function of temperature for the 16-6, 18-12, and 35-6 alloys. Source: Ref 11

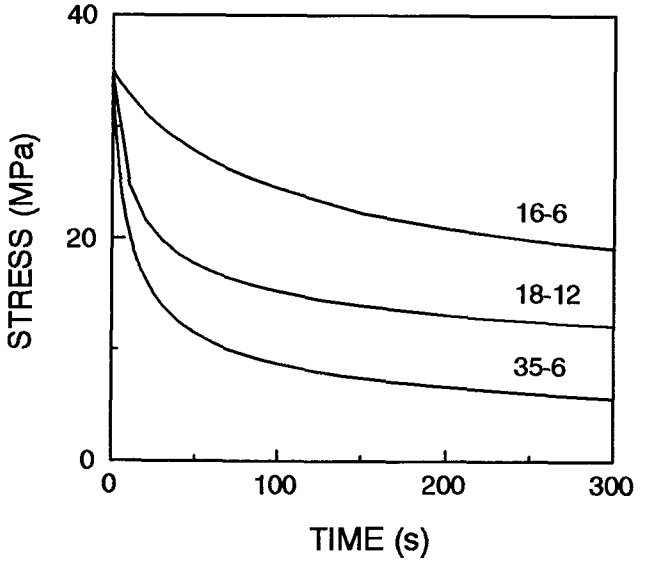

Fig. 6 Calculated 900 °C isothermal stress relaxation curves for 16-6, 18-12, and 35-6 alloys for a starting stress of 35 MPa. Source: Ref 10

Following the procedure shown schematically in Fig. 5, it was not possible to test the alloys at identical starting stresses. Therefore, their stress relaxation behavior could not be directly compared. It was possible, however, to write Euler forward integration equations for each alloy that were very good descriptions of their isothermal stress versus time behavior during stress relaxation (Ref 10). The results of the calculations for a starting stress of 35 MPa and 900 °C are shown in Fig. 6. It is clear that stress relaxation for all three alloys was quite rapid, even for the relatively low starting stress. In fact, relaxation reduced the 35-6 stress to approximately 30% of the starting stress at times of 60 s or less. This time is well within the approximately 240 s that the sample was at the 1150 °C steady-state temperature in the burner rig. Furthermore, relaxation leads to a final stress for the 16-6 alloy that was higher than that for the 35-6 alloy by a factor of three. This calculated relaxation behavior at a constant temperature is similar to relaxation during the steady-state portion of a burner rig cycle. To relate relaxation to TBC life, it is necessary to examine the entire thermal cycle.

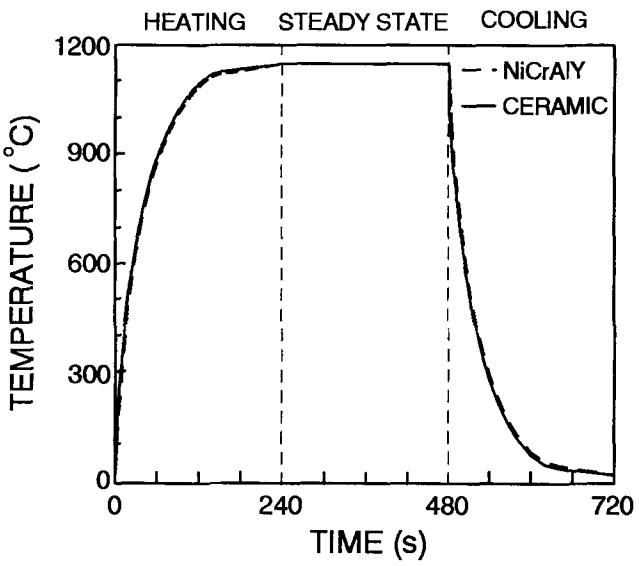

Fig. 7 Temperature versus time profiles for the ceramic and bond coat layers during a burner rig thermal cycle to 1150 °C. The plotted values are average layer temperatures. Source: Ref 9

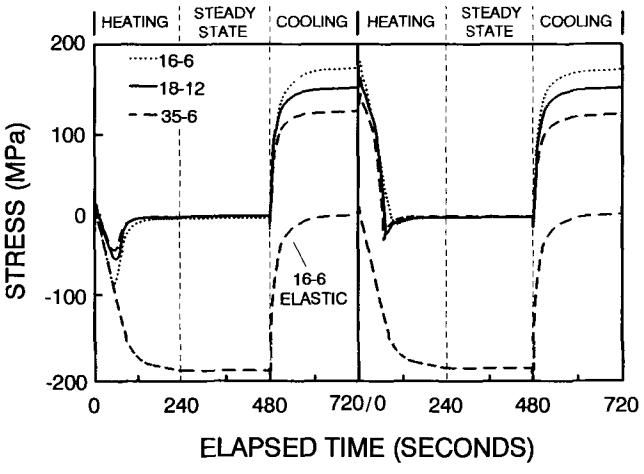

Fig. 8 Calculated ceramic layer out-of-plane stress generated during the first two thermal cycles as a function of time for the 16-6, 18-12, and 35-6 alloys. The lowest curve is for an alloy assumed to have the properties of the 16-6 alloy, except that it was not allowed to relax. Source: Ref 9

3.6 *Stress Relaxation, CTE, and TBC Life*

Identification of the differences in CTE and relaxation behavior among the alloys leads naturally to this question: How do these properties affect TBC life? This has been investigated by expanding the simple forward integration model of stress relaxation developed in the previous section to predict the stresses in the ceramic layer during two burner rig thermal cycles to 1150 °C. The development of the model has been discussed elsewhere (Ref 9). The basic assumptions of the model were that (1) the important stresses driving TBC failure for this burner rig test were out-of-plane tensile stresses generated at the peaks of bond coats (Ref 16-18), (2) the residual stress at the beginning of the first cycle was zero, and (3) the oxidation, ceramic layer creep, and substrate effects could be ignored since they were the same for all three bond coats. The model also included the temperature-dependent properties of the bond coat and realistic temperatures for the bond coat and top coat during a burner rig thermal cycle (Fig. 7) (Ref 7). The assumption used to interpret the data was that TBC life decreases with increasing tensile out-of-plane stresses.

The calculated out-of-plane stress versus time curves for the first two burner rig cycles are shown in Fig. 8. As a point of reference, a stress versus time curve for a 16-6 alloy assumed to deform only elastically is also shown. The most striking feature of Fig. 8 is that there was a dramatic increase in the out-of-plane tensile stress for the bond coats that were allowed to relax as compared to the 16-6 elastic alloy. The conclusion drawn from these data is that bond coats that relax at the use temperature would provide shorter TBC life than a strong alloy that deforms only elastically during a thermal cycle. This conclusion agrees qualitatively with the findings of Wortman et al. (Ref 6), who showed that creep-resistant bond coats provided higher ceramic layer thermal cycle lives than did standard bond coats. It also agrees with the more quantitative finite-element model findings of Petrus and Ferguson (Ref 18) for a rough bond coat/ceramic layer interface.

The second point from Fig. 8 is that the 16-6 bond coat that was allowed to relax exhibited the highest residual tensile stress at the end of the thermal cycles; the 18-12 alloy had the next highest calculated residual stress, and the 35-6 alloy had the lowest. A prediction of TBC life based on the calculated residual stress alone follows the ranking of life determined in the actual burner rig test (Fig. 1) as 35-6 > 18-12 > 16-6.

The relation of calculated residual stress to cyclic life is clearly shown in Fig. 9. The solid line is the regression fit to the cyclic life versus residual stress data, and the dashed lines indicate the 95% confidence interval for the data. Although other factors cannot be strictly ruled out, there appears to be a strong correlation between the cyclic life of a TBC and the calculated residual stress. No other factor, including oxidation behavior, has yet been found to account for the observed differences in TBC life for these three bond coat compositions.

Another feature of Fig. 8 that should be noted is that the residual stress at the end of the first thermal cycle is the same as that at the end of the second thermal cycle, despite the very different starting stresses for the first two cycles. This is related to the high rate of relaxation for these alloys at the steady-state temperature. Obviously, the final stress would not stabilize as readily if the bond coats did not relax to near-zero stress during the steady-state temperature portion of the thermal cycle. A longer time to stabilize the stress may occur for these alloys at lower steady-state temperatures or for more creep-resistant alloys at the 1150 °C steady-state temperature used in this study (Ref 9).

It is now appropriate to revisit the role of CTE in residual stress. For this illustration, only the 16-6 and 35-6 alloys will be examined. Both alloys relax to near-zero stress during steady state at 1150 °C. Thus, out-of-plane tensile stress generation for these alloys occurs only during cooling (Fig. 8). Also, the 35-6 alloy had a higher CTE to 1000 °C than the 16-6 alloy (Fig. 10) and is expected to have a higher average CTE to 1150 °C. Finally, the elastic out-of-plane tensile stress is directly related to the product of the difference in CTE between the ceramic and bond coat (ΔCTE) and the change in temperature (ΔT) as:

$$\sigma \propto \Delta\text{CTE} \cdot \Delta T$$

When ΔT is the same for two different systems, the residual stress scales directly to the ΔCTE. Therefore, in the absence of relaxation, a TBC incorporating the 35-6 alloy would have higher out-of-plane tensile stresses on cooling than would the 16-6 alloy, because the ΔCTE to 1150 °C is higher for the 35-6 alloy than for 16-6 alloy (see Fig. 10). However, relaxation has been calculated for the 35-6 alloy to continue to temperatures as low as 800 °C on cooling, whereas very little relaxation occurred for the 16-6 alloy on cooling (Ref 9). The high-temperature relaxation during cooldown for the 35-6 alloy in effect eliminates the stress generated during the 800 to 1150 °C high CTE portion of the CTE versus temperature curve. The stress for the 35-6 alloy in this case results from an effective ΔCTE much lower than for the 35-6 elastic case and smaller than for the 16-6 alloy (see Fig. 10).

Thus, it is the interaction of stress relaxation with the path of the CTE curve that allows the 35-6 alloy to have lower ceramic layer residual stresses than the 16-6 bond coat, even though the average CTE to 1150 °C is higher than for the 16-6 alloy. The point to remember, then, is that if relaxation of the bond coat is occurring, the path of the CTE versus temperature curve may be more important to the residual stresses than is the average CTE to the maximum temperature. In light of the data, it is too simple to state that stronger bond coats will provide longer TBC lives. Clearly, a very strong bond coat that behaves elastically will give the lowest ceramic layer residual tensile stresses at the end of the thermal cycle (Fig. 8). However, the 16-6 alloy, which was the strongest of the three bond coats examined, had the highest residual stresses, and the weakest bond coat had the lowest residual stresses. It appears from this that there is a minimum in TBC life with increasing bond coat strength, with an absolute maximum at strengths that make the bond coat "creep-proof." Thus, for thermal cycles at temperatures at which all these alloys remain elastic, the lowest overall CTE bond coat may be the best. Designing an optimal bond coat for a TBC requires consideration of the thermal conditions, the bond coat CTE path, and the relaxation behavior of the bond coat.

Although the calculated residual stresses for the three bond coats of this study showed a strong correlation to TBC life, it must be remembered that other factors may be important in determining TBC life. Bond coat oxidation has been clearly linked to TBC life, while interdiffusion with the substrate and other factors are suspected to contribute to TBC degradation. For the special case in this study, where oxidation and other factors were taken into account, it appears that the residual stress, as determined by the stress relaxation and CTE behavior of each alloy, had a significant influence on TBC life.

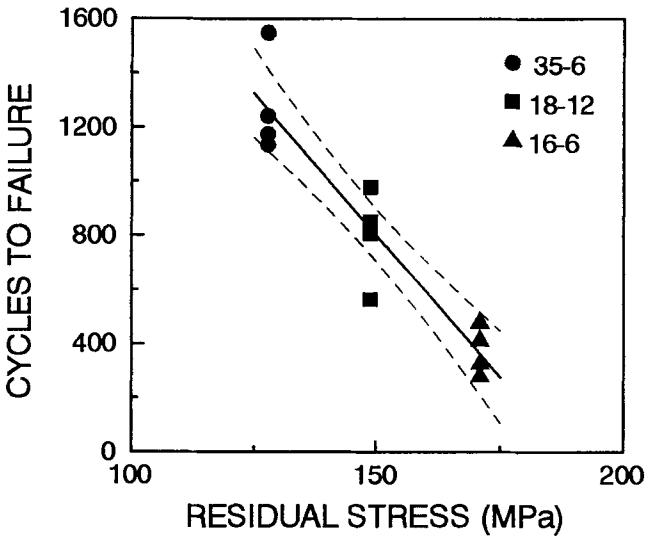

Fig. 9 Measured burner rig thermal cycle life versus the calculated residual stress at the end of a cooling cycle. The solid line shows the regression fit to the data, and the dashed lines indicate the 95% confidence interval for the line. Source: Ref 9

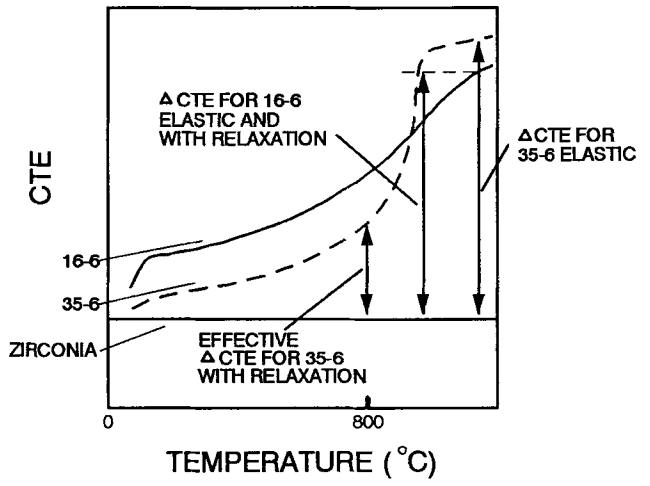

Fig. 10 Schematic of CTE versus temperature comparing the ΔCTE for the 16-6 elastic and with relaxation, the 35-6 elastic, and the effective ΔCTE of the 35-6 as modified by stress relaxation. ΔCTE is the difference in CTE between the bond coat and the zirconia ceramic layer and is directly related to residual stress generation.

4. Summary and Conclusions

The physical and mechanical properties of three LPPS NiCrAlY bond coats with similar oxidation behavior were reviewed with the intent of determining which of these properties were of most importance to TBC life. Although oxidation is still a primary driver of failure, the cyclic life data showed that other factors can significantly affect TBC life. Significant differences in CTE and stress relaxation were found for the three alloys, while the elastic modulus of the alloys was not expected to be important to TBC life. A simple model devised to examine the potential effect of stress relaxation and CTE on TBC life indicated that:

- Stress relaxation of the bond coat for plasma-sprayed coatings is expected to result in significant increases in the out-of-plane residual stresses generated at bond coat peaks as compared to bond coats that do not creep. Since out-of-plane tensile stresses cause delamination of the ceramic layer, stress relaxation of the bond coat is expected to have a deleterious effect on TBC life.
- The calculated residual stresses due to bond coat creep showed a strong correlation to the measured thermal cycle lives of TBCs deposited on the three bond coats. Thus, residual stresses can account for the difference in TBC life for the three alloys, whereas the factors of oxidation and elastic modulus cannot.
- The residual stress considerations presented in this paper were for one thermal cycle condition. It is clear, however, that the residual stresses will depend on steady-state temperature and cooling rates and may depend on heating rates. Thus, bond coat selection is not simply a matter of selecting the bond coat that gives the lowest calculated residual stress for the 1150 °C burner rig cycle of this study. Rather, selection requires consideration of the specific thermal cycle for a given application.

Thermal barrier coating failure is complex and involves numerous factors. For the current study, where oxidation and elastic modulus have been ruled out, the secondary factors such as bond coat roughness and substrate effects have been minimized, there is strong evidence that bond coat stress relaxation and CTE influence TBC failure. Additional factors that generally must be considered in selecting a bond coat include oxidation, bond coat roughness, bond coat quality, differences in oxide strength and oxide adhesion, and possibly others. These factors require further study to determine their effects on TBC life.

Acknowledgments

The author gratefully acknowledges helpful discussions with R.A. Miller and J.G. Goedjen.

References

1. R.A. Miller, Oxidation-Based Model for Thermal Barrier Coating Life, *J. Am. Ceram. Soc.*, Vol 67 (No. 8), 1984, p 517-521
2. W.R. Sevcik and B.L. Stoner, "An Analytical Study of Thermal Barrier Coated First Stage Blades in a JT9D Engine," NASA Contractor Report CR 135360, National Aeronautics and Space Administration, 1978
3. J.T. DeMasi-Marcin, K.D. Sheffler, and S. Bose, "Mechanisms of Degradation and Failure in a Plasma Deposited Thermal Barrier Coating," ASME Paper 89-GT-132, American Society of Mechanical Engineers, 1989
4. S. Rangaswamy, H. Herman, and S. Safai, *Thin Solid Films*, Thermal Expansion Study of Plasma Sprayed Oxide Coatings, Vol 73, 1980, p 43-52
5. M.A. Gedwill, "Improved Bond Coatings for Use with Thermal Barrier Coatings," NASA Tech. Memo. TM-81567, National Aeronautics and Space Administration, 1980
6. D.J. Wortman, E.C. Duderstadt, and W.A. Nelson, "Bond Coat Development for Thermal Barrier Coatings," ASME Paper 89-GT-134, American Society of Mechanical Engineers, 1989
7. W.J. Brindley and R.A. Miller, Thermal Barrier Coating Life and Isothermal Oxidation of Low-Pressure Plasma-Sprayed Bond Coat Alloys, *Surf. Coat. Technol.*, Vol 43-44, 1990, p 446-457
8. R.A. Miller and C.E. Lowell, Failure Mechanisms of Thermal Barrier Coatings Exposed to Elevated Temperatures, *Thin Solid Films*, Vol 95, 1982, p 265-273
9. W.J. Brindley, Bond Coat Stress Relaxation and Thermal Barrier Coating Life, *Mater. Sci. Eng.*, submitted for publication
10. W.J. Brindley and J.D. Whittenberger, Stress Relaxation of Low Pressure Plasma Sprayed NiCrAlY Alloys, *Mater. Sci. Eng.*, Vol A163, 1993, p 33-41
11. L.S. Cook, A. Wolfenden, and W.J. Brindley, Temperature Dependence of Dynamic Young's Modulus and Internal Friction in LPPS NiCrAlY, *J. Mater. Sci.*, Vol 29, 1994, p 5104-5108
12. P.A. Siemers and R.L. Mehan, Mechanical and Physical Properties of Plasma-Sprayed Stabilized Zirconia, *Ceram. Eng. Sci. Proc.*, Vol 4 (No. 9/10), 1983, p 828-840
13. R.V. Hillery, B.H. Pilsner, R.L. McKnight, T.S. Cook, and M.S. Hartle, "Thermal Barrier Coating Life Prediction Model Development," NASA Contractor Report 180807, National Aeronautics and Space Administration, 1988
14. M.G. Hebsur and R.V. Miner, Stress Rupture and Creep Behavior of a Low Pressure Plasma-Sprayed NiCoCrAlY Coating Alloy in Air and Vacuum, *Thin Solid Films*, Vol 147, 1987, p 143-152
15. J.M. Veys, A. Riviere, and R. Mevrel, Mechanical Properties of LPPS NiCoCrAlYTa, *Proc. First Plasma Technik Symp.*, Vol 2, H. Eschnauer, P. Huber, A.R. Nicoll, and S. Sandmeier, Ed., Plasma Technik AG, Wohlen, Switzerland, 1988, p 115-124
16. A.G. Evans, G.B. Crumley, and R.E. Demaray, On the Mechanical Behavior of Brittle Coatings and Layers, *Oxid. Met.*, Vol 20 (No. 5/6), 1983, p 193-216
17. W. Phucharoen, "Development of an Analytical-Experimental Methodology for Predicting the Life and Mechanical Behavior of Thermal Barrier Coatings," Ph.D. dissertation, Cleveland State University, 1990
18. G. Petrus and B.L. Ferguson, A Software Tool to Design Thermal Barrier Coatings, *Proc. Thermal Barrier Coating Workshop*, NASA Lewis Research Center, 1994